

## Fullerene as a Probe Molecule for Single-Atom Oxygen Reduction Electrocatalysts

Ning Li<sup>#a</sup>, Kun Guo<sup>\*\*a</sup>, Song Lu<sup>b</sup>, Lipiao Bao<sup>a</sup>, Zhixin Yu<sup>c</sup>, and Xing Lu<sup>\*a</sup>

<sup>a</sup>*State Key Laboratory of Materials Processing and Die & Mould Technology, School of Materials Science and Engineering, Huazhong University of Science and Technology, Wuhan 430074, China*

<sup>b</sup>*Institute of New Energy, School of Chemistry and Chemical Engineering, Shaoxing University, Shaoxing 312000, China*

<sup>c</sup>*Department of Energy and Petroleum Engineering, University of Stavanger, Stavanger 4036, Norway*

<sup>#</sup>These authors contributed equally to this work.

\*Corresponding author:

K. Guo ([guok@hust.edu.cn](mailto:guok@hust.edu.cn))

X. Lu ([lux@hust.edu.cn](mailto:lux@hust.edu.cn))

## Table of Contents

<b>Experimental Section</b> .....	3
<b>Figure S1.</b> Polarization plots of ORR on various MP/CNT (M = Fe, Mn, Ni, Co) with a MP loading of 50 wt.% and their corresponding $E_{1/2}$ values in 0.1 M KOH at 1600 rpm. ....	6
<b>Figure S2.</b> Polarization plots of ORR on various CoP/CNT with CoP:CNT mass ratios of 1:4, 1:2, 1:1, 4:1 and their corresponding $E_{1/2}$ values in 0.1 M KOH at 1600 rpm.....	7
<b>Figure S3.</b> SEM and TEM images of CNT (a,b), CoP/CNT (c,d), and C <sub>60</sub> -CoP/CNT (e,f).....	8
<b>Figure S4.</b> Full-survey XPS spectra of CoP, CoP/CNT, and C <sub>60</sub> -CoP/CNT. ....	9
<b>Figure S5.</b> HO <sub>2</sub> <sup>-</sup> yield and electron transfer number ( $n$ ) value derived from the rotating ring-disk electrode test of CoP/CNT.....	10
<b>Figure S6.</b> Geometric configurations of C <sub>60</sub> adsorbed to carbon-supported CoP without (a) and with (b) an O <sub>2</sub> molecule bound to the Co site. The spatial distances between Co atom and a C atom in the bottom pentagon of C <sub>60</sub> are indicated. Color code: C, cyan; N, blue; H, white; Co, green; O, black. ....	11
<b>References</b> .....	12

## Experimental Section

### 1. Chemicals

All chemicals were purchased and used as received without further treatment unless otherwise indicated. C<sub>60</sub> fullerene (99%) was purchased from Xiamen Funano New Material Technology Co., Ltd. Cobalt(II) meso-tetraphenylporphine (CoP, 98%), nickel(II) meso-tetraphenylporphine (NiP, 97%), iron(III) meso-tetraphenylporphine chloride (FeP, 95%), and (5,10,15,20-tetraphenylporphinato) manganese(III) chloride (MnP, 95%) were bought from Shanghai Aladdin Biochemical Technology Co., LTD. Potassium hydroxide (KOH, ≥85.0%), potassium thiocyanate (KSCN, ≥98.5%), and carbon disulfide (CS<sub>2</sub>, 99.9%) were ordered from Sinopharm Chemical Reagent Co., Ltd. Carbon nanotube (CNT, multi-walled, 95%, length of 10–30 μm and diameter of 10–20 nm) was received from Nanjing XFNANO Materials Tech Co., Ltd. Ketjenblack EC-600 JD (KB) was ordered from AkzoNobel. Nafion ionomer solution (5 wt%) was obtained from Sigma Aldrich. Deionized water (18.2 MΩ·cm) was used in all the experiments.

### 2. Materials Synthesis

#### Synthesis of CNT-supported metalloporphyrins (MP/CNT)

Taking the synthesis of CoP/CNT as an example, 20 mg of CoP was dissolved in 10 mL of CS<sub>2</sub> to form a homogeneous solution, into which 20 mg of CNT was thoroughly dispersed by ultrasonication for 2 h. The final product was then received by vacuum rotary evaporation at 80 °C and a rotating speed of 400 rpm to remove CS<sub>2</sub>. NiP/CNT, FeP/CNT, and MnP/CNT were prepared by simply replacing CoP with the same mass of NiP, FeP, and MnP, respectively.

#### Synthesis of C<sub>60</sub>-adsorbed MP/CNT

C<sub>60</sub>-CoP/CNT was synthesized by dissolving 20 mg of CoP and 22 mg of C<sub>60</sub> in 10 mL of CS<sub>2</sub> to form a homogeneous solution, into which 20 mg of CNT was thoroughly dispersed by ultrasonication for 2 h. The final product was then received by vacuum rotary evaporation at 80 °C and a rotating speed of 400 rpm to remove CS<sub>2</sub>. C<sub>60</sub>-NiP/CNT was prepared by simply replacing CoP with the same mass of NiP.

### 3. Material Characterization

Transmission electron microscopy (TEM) was carried out on a JEM-2010F (JEOL) electron microscope at an accelerating voltage of 200 kV. A copper grid coated with a thin carbon film was used

as the specimen holder. Scanning electron microscopy (SEM) was performed on a Nova NanoSEM 450 (FEI) electron microscope at an accelerating voltage of 10 kV.

X-ray powder diffraction (XRD) was performed to obtain the crystallographic information of the samples. The powder diffraction patterns were recorded on a Malvern Panalytical X-ray diffractometer (Empyrean) using Cu K $\alpha$  radiation source ( $\lambda = 1.5406 \text{ \AA}$ , 45 kV and 40 mA). Scanning angles for all samples were set in the  $2\theta$  range of  $5\text{--}90^\circ$  with a step size of  $0.01313^\circ$  and time per step of 120 s. Peaks were indexed to the database established by Joint Committee on Powder Diffraction Standards (JCPDS).

Raman spectrum was acquired using a confocal Raman microscope (LabRAM HR800, Horiba JobinYvon) equipped with an optical microscope, a CCD camera, and an argon ion laser source. The laser provided 0.2 mW power at a wavelength of 532 nm for the exciting line. Integration time was 60 s, number of co-addition was 2, and slit aperture size was  $50 \times 1000 \text{ }\mu\text{m}$ .

X-ray photoelectron spectroscopy (XPS) analysis was performed on the K-Alpha X-ray photoelectron spectrometer system (Thermo Fisher Scientific) utilizing a monochromatic Al K $\alpha$  source (1486.69 eV). High-resolution spectra were obtained at a pass energy of 50.0 eV, a step size of 0.1 eV, and a dwell time of 250 ms per step. The analysis spot size was  $400 \text{ }\mu\text{m}$ . All binding energies were calibrated to the graphitic C 1s peak at 284.8 eV. XPS peaks were deconvolved and curve-fitted on the CasaXPS software using the Lorentzian function and Shirley background.

#### 4. Electrochemical Measurements

Electrochemical measurements were conducted on a CHI760E electrochemical workstation (Shanghai Chenhua Instruments Co., Ltd., China) and a MSR rotator (Pine Instrument Company, USA) in a standard three-electrode cell at room temperature ( $25 \text{ }^\circ\text{C}$ ). A glassy carbon rotating disk electrode (RDE, diameter of 5 mm), an Ag/AgCl in saturated KCl electrode, and a platinum foil were used as the working, reference, and counter electrodes, respectively. All potentials were calibrated to the reversible hydrogen electrode (RHE) according to the Nernst equation  $E_{\text{vs RHE}} = E_{\text{vs Ag/AgCl}} + 0.198 + 0.0592 \times \text{pH}$ . 0.1 M KOH aqueous solution with a pH value of 13 was used as the electrolyte.

The working electrode was fabricated via the following procedures: 5 mg of the as-prepared catalyst was dispersed in a mixture of 960  $\mu\text{L}$  of ethanol and 40  $\mu\text{L}$  of 5 wt % Nafion solution. The mixture was ultrasonically dispersed for at least 0.5 h to obtain a homogeneous suspension. Then 20  $\mu\text{L}$  of the

suspension was taken by a microsyringe and drop-casted onto a clean RDE with an overall loading of  $0.25 \text{ mg cm}^{-2}$ . The modified RDE was dried naturally in air. Prior to the tests, the electrochemical cell was saturated by purging  $\text{N}_2$  or  $\text{O}_2$  for at least 30 min. The linear sweep voltammetry (LSV) scan potential was set from 1.2 to 0 V, the scan rate was  $10 \text{ mV s}^{-1}$ , and the rotational speeds were 400–1600 rpm. In the  $\text{SCN}^-$  poisoning experiment, the working electrode with CoP/CNT was immersed in 0.01 M KSCN solution for 2 h. The immersed electrode was then immediately tested by LSV in  $\text{O}_2$ -saturated 0.1 M KOH to avoid the slow reaction between  $\text{SCN}^-$  and KOH.

The rotating ring-disk electrode (RRDE) measurements were conducted in  $\text{O}_2$ -saturated 0.1 M KOH at 1600 rpm and a scan rate of  $10 \text{ mV s}^{-1}$ . The ring potential was set as 1.3 V. The  $n$  value and peroxide yield ( $\text{HO}_2^-$ ) were calculated by the following equations:

$$\text{HO}_2^-(\%) = 200 \times \frac{I_r/N}{I_d + I_r/N} \#(1)$$

$$n = 4 \times \frac{I_d}{I_d + I_r/N} \#(2)$$

where  $I_r$  and  $I_d$  are the ring and disk currents, respectively, and  $N$  is the current collection efficiency of RRDE (0.37).

## 5. Theoretical Calculation Details

All the density functional theory (DFT) calculations were conducted with the projector-augmented wave method implemented in the Vienna *ab initio* Simulation Package (VASP).<sup>[S1,2]</sup> The implicit solvent model was included by VASPsol.<sup>[S3]</sup> Atomic models, including  $\text{C}_{60}$  on the same side and opposite sides of a CoP molecule that is pre-stabilized on intact graphene were built for corresponding investigations. A  $8 \times 4 \times 1$  sized supercell consisting of 128 carbon atoms was used as the graphene-based matrix. Periodic boundary conditions and a supercell with a separation of about  $14 \text{ \AA}$  were used to ensure that the interactions between adjacent supercells were negligible. Meanwhile, a vacuum of  $15 \text{ \AA}$  was imposed in the  $Z$  direction. The Perdew-Burke-Ernzerhof (PBE) within the generalized gradient approximation (GGA) was employed as an exchange-correlation functional.<sup>[S4]</sup> A plane-wave cutoff energy of 450 eV was chosen for all the computations to describe all atoms' valence electrons. The convergence criterion of energy and force was set to  $10^{-4} \text{ eV}$  and  $0.02 \text{ eV \AA}^{-1}$ , respectively. The van der Waals (vdW) interactions were described by the Grimme's scheme (DFT-D3) correction method.<sup>[S5]</sup>



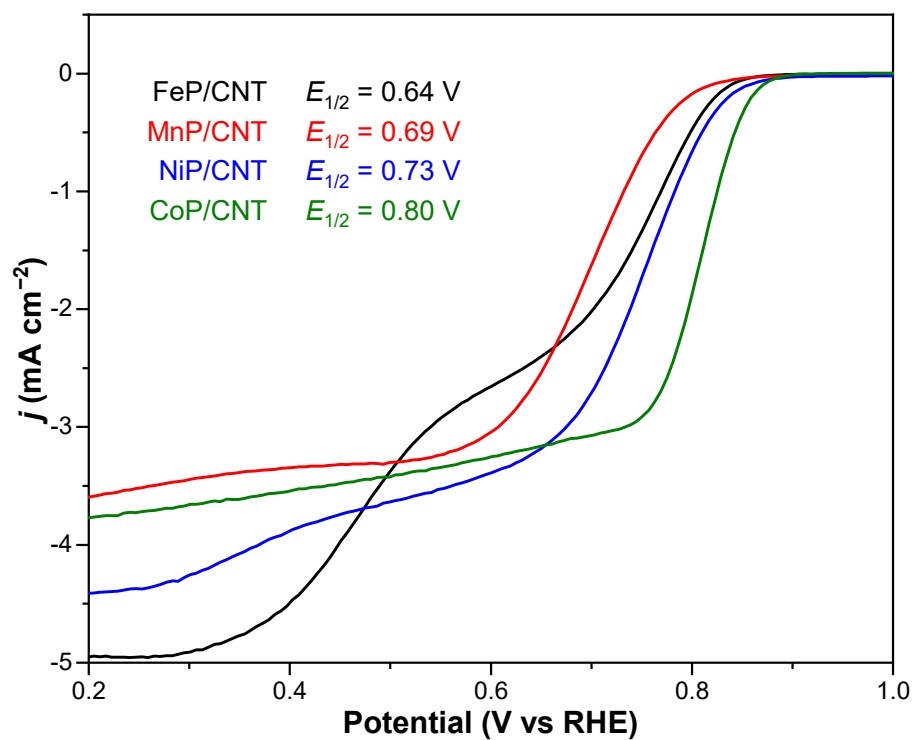


**Figure S1.** Polarization plots of ORR on various MP/CNT (M = Fe, Mn, Ni, Co) with a MP loading of 50 wt.% and their corresponding  $E_{1/2}$  values in 0.1 M KOH at 1600 rpm.

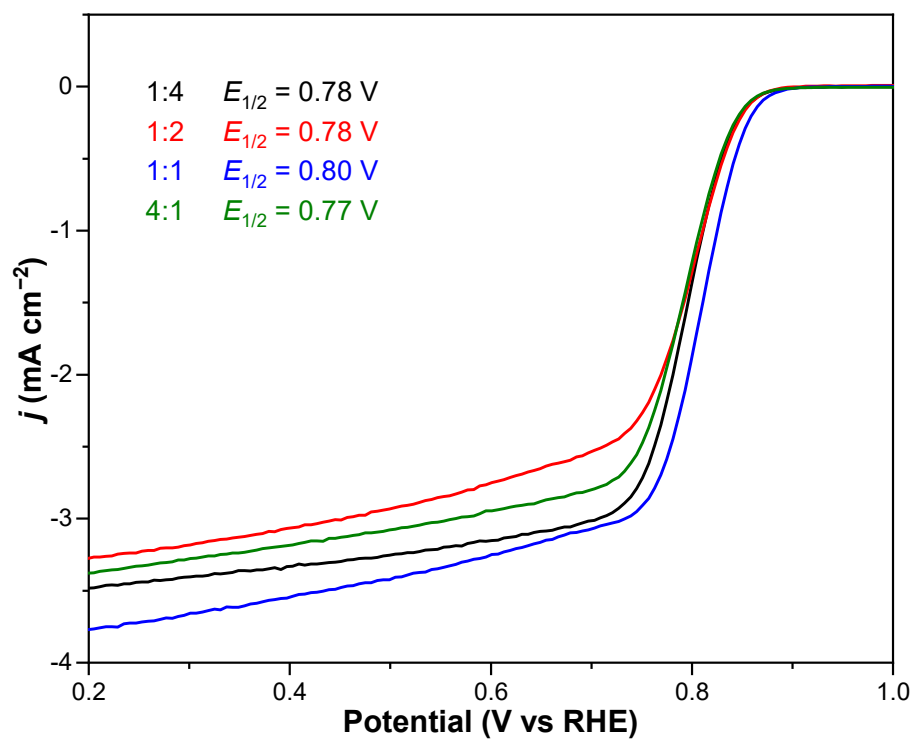


**Figure S2.** Polarization plots of ORR on various CoP/CNT with CoP:CNT mass ratios of 1:4, 1:2, 1:1, 4:1 and their corresponding  $E_{1/2}$  values in 0.1 M KOH at 1600 rpm.



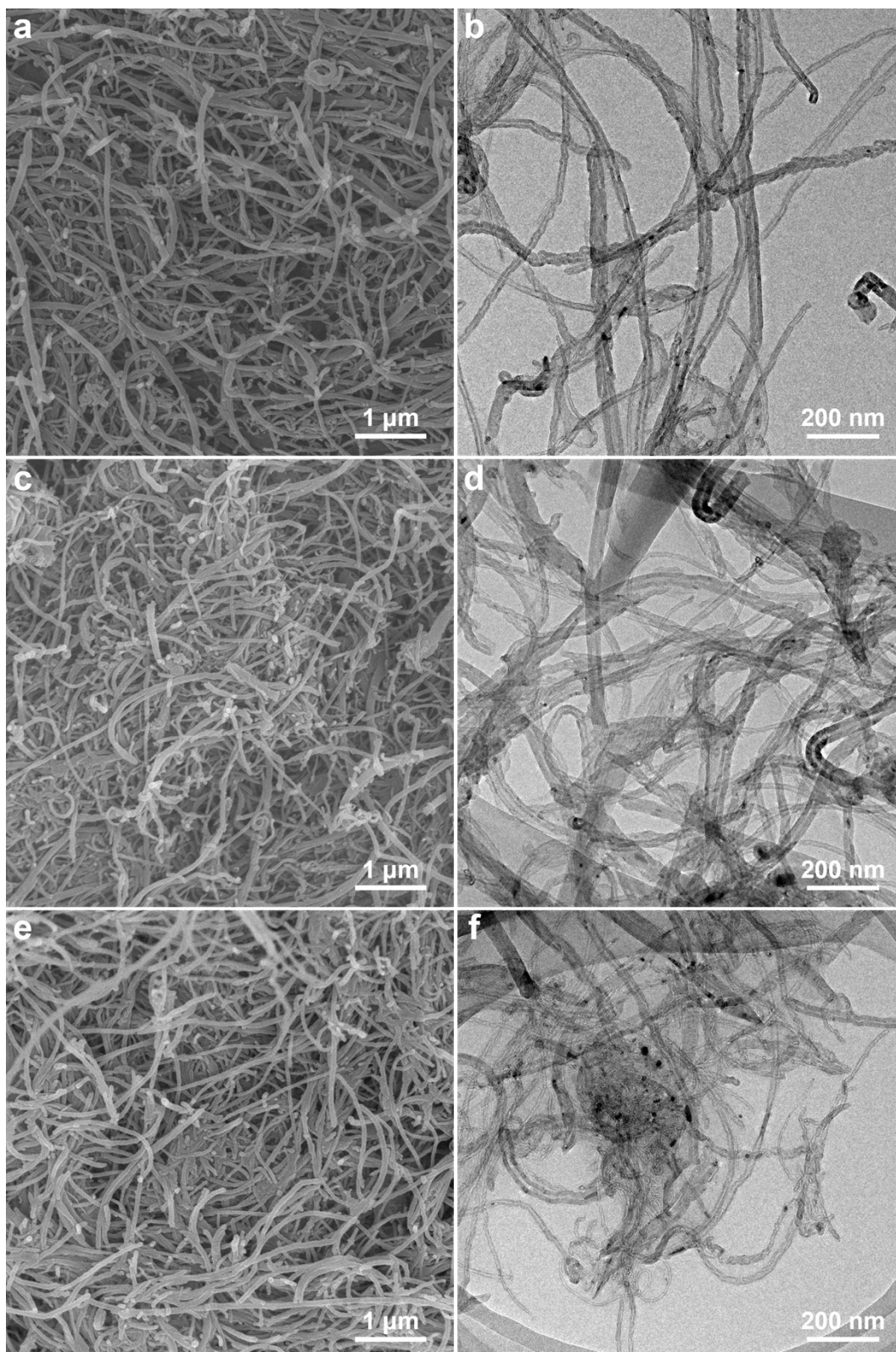


**Figure S3.** SEM and TEM images of CNT (a,b), CoP/CNT (c,d), and C<sub>60</sub>-CoP/CNT (e,f).

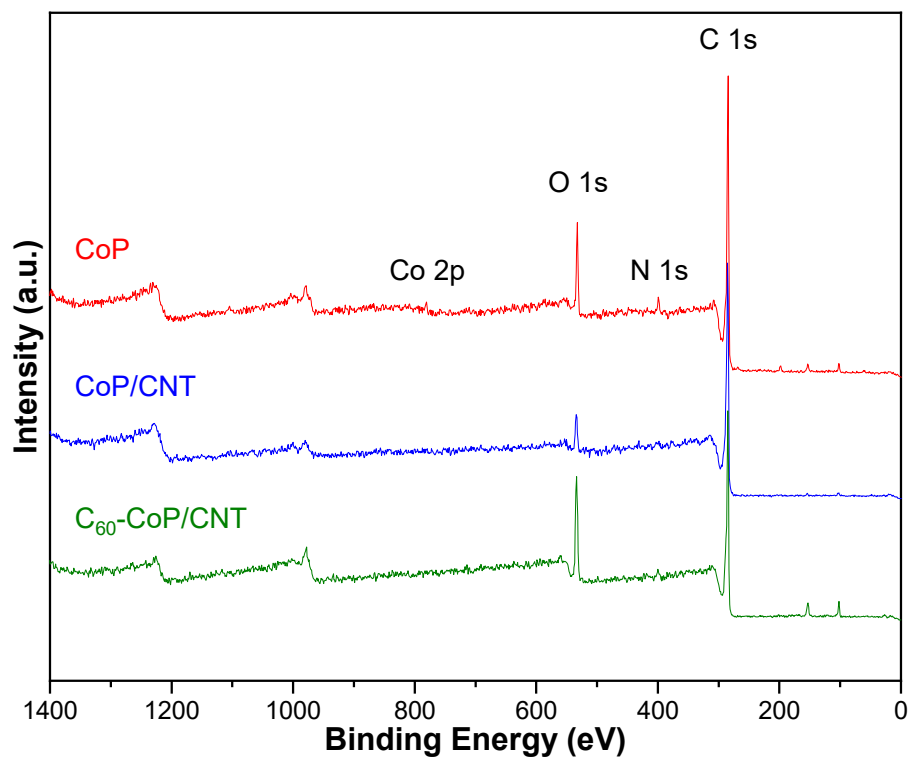


**Figure S4.** Full-survey XPS spectra of CoP, CoP/CNT, and C<sub>60</sub>-CoP/CNT.

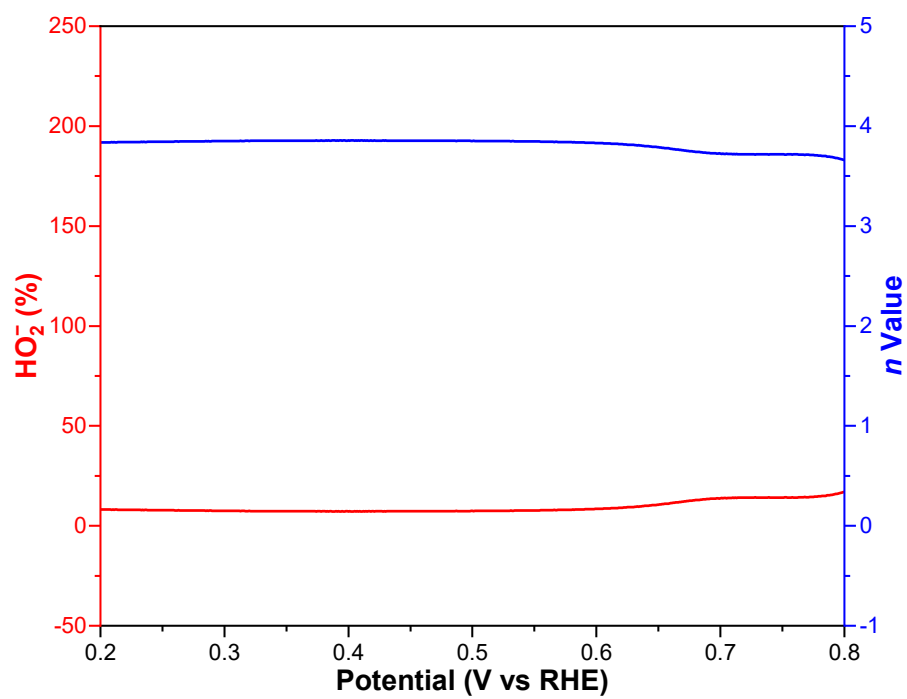


**Figure S5.** HO<sub>2</sub><sup>-</sup> yield and electron transfer number (*n*) value derived from the rotating ring-disk electrode test of CoP/CNT.

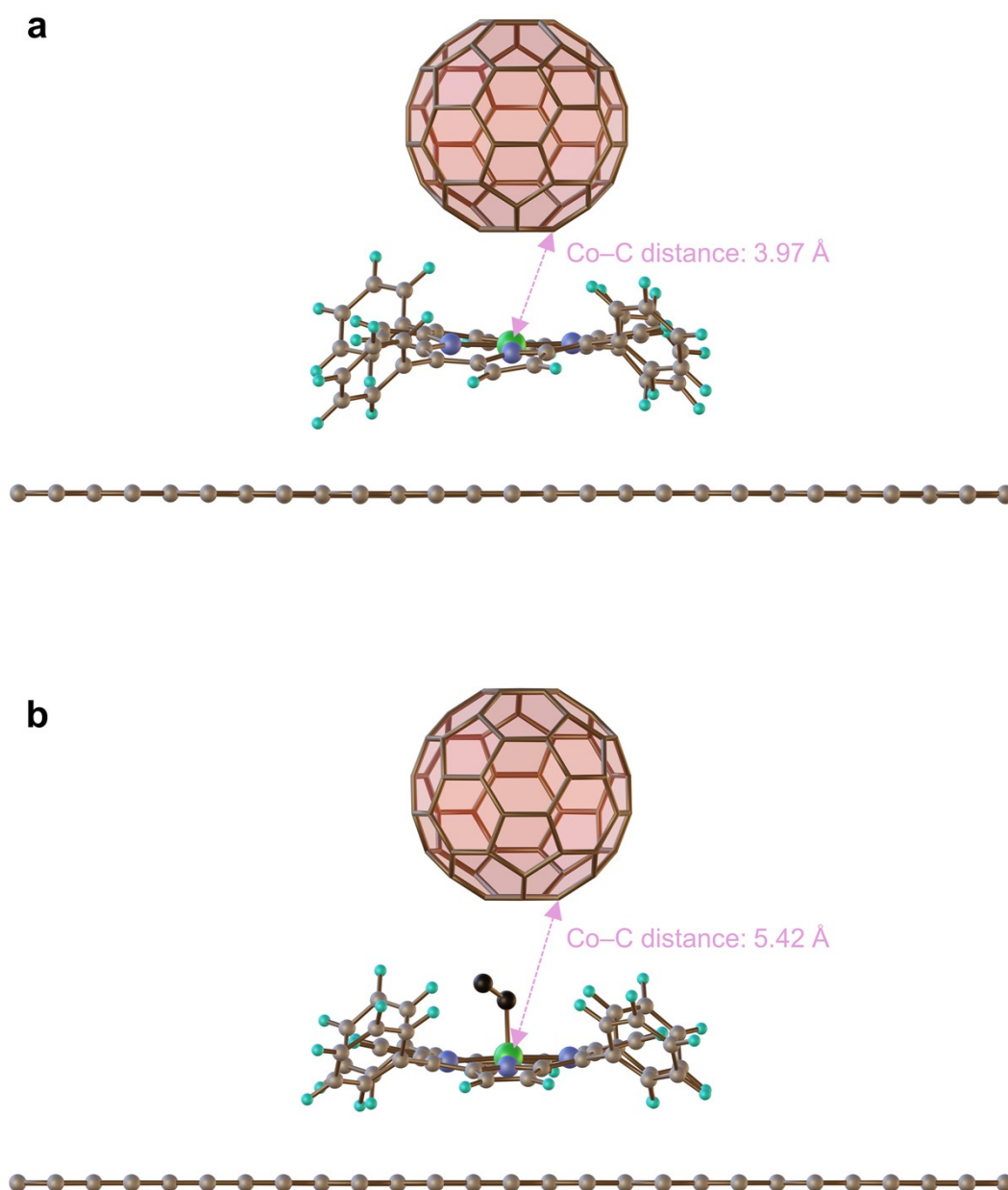


**Figure S6.** Geometric configurations of  $C_{60}$  adsorbed to carbon-supported CoP without (a) and with (b) an  $O_2$  molecule bound to the Co site. The spatial distances between Co atom and a C atom in the bottom pentagon of  $C_{60}$  are indicated. Color code: C, cyan; N, blue; H, white; Co, green; O, black.

The extended spatial distance between Co atom and  $C_{60}$  molecule after  $O_2$  adsorption indicates that steric hindrance is created after  $C_{60}$  adsorption such that  $O_2$  molecules will have to overcome the considerable interactions between  $C_{60}$  and CoP to be able to approach the central Co atom.

## References

[S1] G. Kresse, J. Furthmuller, *Phys. Rev. B* **1996**, *54*, 11169.

[S2] G. Kresse, D. Joubert, *Phys. Rev. B* **1999**, *59*, 1758.

[S3] K. Mathew, R. Sundararaman, K. Letchworth-Weaver, T.A. Arias, R.G. Hennig, *J. Chem. Phys.* **2014**, *140*, 084106.

[S4] J.P. Perdew, K. Burke, M. Ernzerhof, *Phys. Rev. Lett.* **1996**, *77*, 3865.

[S5] S. Grimme, J. Antony, S. Ehrlich, H. Krieg, *J. Chem. Phys.* **2010**, *132*, 154104.